This article has not been copyedited and formatted. The final version may differ from this version.
JPET Fast Forward. Published on January 6, 2012 as DOI: 10.1124/jpet.111.187740

JPET #187740

RN486 [6-Cyclopropyl-8-fluoro-2-(2-hydroxymethyl-3-{1-methyl-5-[5-(4-methyl-piperazin-1-yl)-pyridin-2-ylamino]-6-oxo-1,6-dihydro-pyridin-3-yl}-phenyl)-2H-isoquinolin-1-one], a Selective Bruton's Tyrosine Kinase (Btk) Inhibitor, Abrogates Immune Hypersensitivity Responses and Arthritis in Rodents

Daigen Xu, Yong Kim, Jennifer Postelnek, Minh Diem Vu, Dong-Qing Hu, Cheng Liao, Mike Bradshaw, Jonathan Hsu, Jun Zhang, Achal Pashine, Dinesh Srinivasan, John Woods, Anita Levin, Alison O'Mahony, Timothy D. Owens, Yan Lou, Ronald J. Hill, Satwant Narula, Julie DeMartino, and Jay S. Fine

Department of Inflammation Discovery (D.X., Y.K., J.P., M.D.V, D. H., J.H., C.L., J.Z., A.P., D.S., J.W., R.J.H., J.D., J.S.F.), Inflammation Chemistry (T.D.O., Y.L.), Hoffmann-La Roche, Inc., 340 Kingsland Street, Nutley, New Jersey 07110; Principia Biopharma, 525 Del Rey Avenue, Sunnyvale, CA 94084 (Current Address for M.B. and R.J.H); Five Prime Theraputics, Inc., Two Corporate Drive, South San Francisco, CA 94080 (Current Address for A.L.); BioSeek LLC., 310 Utah Avenue, Suite 100, South San Francisco, CA 94080 (AO)

JPET Fast Forward. Published on January 6, 2012 as DOI: 10.1124/jpet.111.187740
This article has not been copyedited and formatted. The final version may differ from this version.

JEPT #187740

Running title page(s)

a). Running title: Btk inhibitors for rheumatoid arthritis

b). Corresponding author:

Daigen Xu, MD; PhD

Inflammation Discovery, PRED

Hoffmann-la-Roche

340 Kingsland Street

Nutley, NJ 07110

Telephone: (973)235-5143

Fax: (973)235-6200

c). Manuscript information

The manuscript contains :

41 text pages

2 tables

9 figures

37 references (40 max)

238 words in Abstract (250 max)

643 words in Introduction (750 max)

1497 words in Discussion (1500 max)

d). ABBREVIATIONS: AAALAC, Association for the Assessment and Accreditation of Laboratory Animal Care International; ABL-1, c-abl oncogene 1, non-receptor tyrosine kinase; ACR, American College of Rheumatologists; AIA, adjuvant-induced arthritis; BCR, B cell antigen receptor; BSA, bovine serum albumin; Btk, Bruton's

tyrosine kinase; CFA, complete Freund's adjuvant; CIA, collagen-induced arthritis; CRP, C reactive protein; Cyp, cyproheptadine; Dex, dexamethasone; DAP12, DNX adaptor protein of 12 kd; EIA, enzyme immunoassay; ELISA; enzyme-linked immunoasorbent assay; FACS, fluorescence activated cell sorter; FBS, fetal bovine serum; FcR, Fc receptor; FGR, tyrosine-protein kinase Fgr; FLIPR, fluorometric imaging plate reader; HSC, hematopoietic stem cell; IFA, incomplete Freund's adjuvant; ITAM, immunoreceptor tyrosine activation motif; ITK, IL2-inducible T-cell kinase; Jak, janus kinase; LCK, lymphocyte-specific protein tyrosine kinase; LPS, lipopolysaccharide; MTX, methotrexate; OVA, ovalbumin; PBMC, peripheral blood mononuclear cell; PCA, passive cutaneous anaphylaxis; PLCγ2, phopholipase C gamma 2; RA, rheumatoid arthritis; RANKL, receptor activator of NF-kappa-B ligand; RANTES, chemokine (C-C motif) ligand 5; rPAR, reverse passive Arthurs' reaction; SCF, stem cell factor; SLK, Ste20 like kinase; Src, sarcoma kinase; Syk, spleen tyrosine kinase; Tmax, time point with maximal blood concentration of test compound; TEC, Tec non receptor kinase; TIMP-1, tissue inhibitor of metalloprotease 1; TR-FRET, time resolved fluorescence resonance energy transfer; VCAM, vascular cell adhesion molecule; YES, Yamaguchi sarcoma viral (v-yes) oncogene homolog 1 (kinase)

e). Recommended section: Inflammation, Immunopharmacology, and Asthma

Abstract

Genetic mutation and pharmacological inhibition of Bruton's tyrosine kinase (Btk) have both been shown to prevent the development of collagen-induced arthritis (CIA) in mice, providing a rationale for the development of Btk inhibitors for treating rheumatoid arthritis (RA). In the present study, we characterized a novel Btk inhibitor RN486 in vitro and in rodent models of immune hypersensitivity and arthritis. We demonstrated that RN486 not only potently and selectively inhibited the Btk enzyme, but also displayed functional activities in human cell-based assays in multiple cell types, blocking FcεR crosslinking-induced degranulation in mast cells (IC_{50}=2.9 nM), FcγR engagement-mediated TNFα production in monocytes (IC_{50}=7.0 nM) and B cell receptor (BCR)-induced expression of an activation marker CD69 in B cells in whole blood (IC_{50}=21.0 nM). RN486 displayed similar functional activities in rodent models, effectively preventing type I and type III hypersensitivity responses. More importantly, RN486 produced robust anti-inflammatory and bone protective effects in mouse CIA and rat adjuvant-induced arthritis (AIA) models. In the AIA model, RN486 inhibited both joint and systemic inflammation either alone or in combination with methotrexate, reducing both paw swelling and inflammatory markers in the blood. Together, our findings not only demonstrate that Btk plays an essential and conserved role in regulating immunoreceptor-mediated immune responses in both humans and rodents, but also provide evidence and mechanistic insights to support the development of selective Btk inhibitors as small molecule disease modifying drugs for RA and potentially other autoimmune diseases.

Introduction

Rheumatoid arthritis (RA) is an autoimmune joint disease characterized by chronic synovial inflammation and progressive joint destruction. The disease is often associated with appearance of autoantibodies in both blood and inflamed joints. Several of these autoantibodies have emerged as potential arthritogenic factors. For example, anti-glucose-6 phosphate isomerase and anti-type II collagen antibodies, both of which are highly arthritogenic in mice, can be detected in RA patients (Schaller, et al., 2005; Mullazehi, et al., 2007). In addition, anti-citrullinated protein autoantibodies, the most prevalent in RA, can bind citrullinated fibrinogen in RA joints to form immune complexes (Zhao, et al., 2008), which stimulate macrophages to produce inflammatory cytokines such as TNFα (Clavel, et al., 2008). Lastly, clinical efficacy of B cell depleting agents in RA strongly implicates autoantibodies as culprits in the pathogenesis of the disease (Edwards, et al., 2005).

The production and effector function of antibodies are regulated by distinct immunoreceptors on B cells and innate immune cells (Kurosaki, 2000; Nimmerjahn and Ravetch, 2008). The receptors, termed B cell antigen receptor (BCR) and activating Fc receptors (FcR), belong to a family of immunoglobulin like immunoreceptors containing an intracellular immunoreceptor tyrosine based activation motif (ITAM) (Kurosaki, 2000; Nimmerjahn and Ravetch, 2008). ITAMs act to integrate diverse antigen- or Fc-specific signals into a common pathway regulated by non-receptor tyrosine kinases including Lyn, spleen tyrosine kinase (Syk) and Bruton's tyrosine kinase (Btk) from the sarcoma kinase (SRC), Syk and Tec kinase families. These kinases relay the signals sequentially from ITAMs to phospholipase C gamma 2 (PLCγ2) (Kurosaki, et al., 2000) and thus play a

critical and non-redundant role in the signal transduction of BCR and FcR. Consequently, loss of function mutation in the Btk gene results in severe B cell immunodeficiency and impaired FcR function in both patients with X-linked agammaglobulinemia and mutant mice with X-linked immunodeficiency (Thomas, et al., 1993; Conley, et al., 1994).

Btk also regulates signaling of other ITAM containing receptors or adaptors, e.g. DNAX-activating protein of 12 kd or DAP12 (Koga, et al., 2004). DAP12 functions as an adaptor protein for multiple receptors, including receptor for macrophage colony stimulating factor (CSF1R) and myeloid DAP12-associating lectin-1 (MDL-1). Both receptors have been implicated in the development of immune arthritis (Huang, et al., 2009; Joyce-Shaikh, et al., 2010). Also importantly, CSF1R, along with FcγR, provides a secondary but indispensable signal for RANKL to promote osteoclast differentiation, and subsequently, bone resorption (Koga, et al., 2004).

Together, Btk and Syk regulate the signal transduction of ITAM containing receptors or adaptors that are critical for autoantibody production, effector function and osteoclast differentiation. Therefore, pharmacological inhibition of these enzymes may impact multiple steps in the pathogenesis of RA and represent a useful approach for the treatment of the disease. Indeed, R788 (fostamatinib), a first generation Syk inhibitor, has been shown to have benefits in both animal models of immune arthritis and in RA patients (Weinblatt, et al., 2010), supporting the concept that inhibitors of Syk and its downstream kinase Btk may have utilities as RA therapeutics. Indeed, emerging evidence demonstrates that inhibition of Btk in mice confers resistance to CIA (Di Paolo, et al., 2011; Honigberg, et al., 2010; Liu, et al., 2011), similarly to Btk mutation (Jansson and Holmdahl, 1993).

JPET Fast Forward. Published on January 6, 2012 as DOI: 10.1124/jpet.111.187740
This article has not been copyedited and formatted. The final version may differ from this version.

In the present study, we characterized a novel, potent and selective reversible Btk inhibitor RN486 in multiple mechanistic as well as disease related cellular assays and animal models. We demonstrated that RN486 inhibited immune responses mediated by two important immunoreceptors, BCR and FcR, in both human cells and rodents. Importantly, RN486 produced dose-dependent efficacy in both CIA and AIA, with evidence for substantial efficacy in combination with low dose methotrexate. These findings support the emerging concept that Btk plays a mandatory role in regulating immunoreceptor signaling in both human and rodents, and suggest the potential utility of selective Btk inhibitors for the treatment of RA and other autoimmune diseases.

JPET Fast Forward. Published on January 6, 2012 as DOI: 10.1124/jpet.111.187740
This article has not been copyedited and formatted. The final version may differ from this version.

Methods

Enzymatic activity and binding assays

Btk enzymatic activity assay. A Caliper fluorescence-based kinase assay was used to measure Btk kinase activity and its inhibition by RN486. In the assay, test compound was incubated with a human recombinant Btk (10 nM), ATP (100 μM) and a fluorescent labeled peptide substrate (15 μM) at 30 ºC for 15 min. The reaction was then stopped by the addition of a termination buffer and reaction product quantified by using a Desktop Profiler 4 sipper (Caliper, Hopkinton, MA).

Time resolved fluorescence resonance energy transfer (TR-FRET) based competitive binding assay. The assay was used to determine the ability of RN486 to competitively inhibit binding of a substrate to Btk. It was adapted from a standard "one step, mix-and-read, TR-FRET binding assay" from Invitrogen (Carlsbad, CA). Briefly, BTK-BioEase™, a biotinylated BTK, was conjugated to a FRET donor europium through an incubation with Eu- Streptavidin (Perkin Elmer, Waltham, MA) for 1 h in a buffer containing 20 mM HEPES (pH 7.15), 0.1 mM DTT, 10 mM $MgCl_2$ and 0.5 mg/ml BSA. BTK-Eu conjugate (0.1 nM) was then incubated with KT-178, a kinase tracer and FRET acceptor from Invitrogen (Carlsbad, CA), and RN486 or vehicle (DMSO) overnight at 15°C. Photons emitted from both the donor (620 nm) and acceptor (FRET, 665 nm) were measured by using a BMG Pherastar Fluorescent plate reader (BMG Labtech Gmbh, Offenberg, Germany). Ratio between the 620 nm and 665 nm signals was calculated to determine Btk-substrate binding and its inhibition by RN486.

Kinomescan selectivity assay. Selectivity of RN486 for Btk over non-Btk kinases was determined by testing the compound at a single 10 μM concentration against

JPET Fast Forward. Published on January 6, 2012 as DOI: 10.1124/jpet.111.187740
This article has not been copyedited and formatted. The final version may differ from this version.

a panel of 396 kinases at Ambit Biosciences (San Diego, CA) using a high throughput Kinomescan based on ATP free competitive binding (Fabian, et al., 2005). RN486 was further titrated against individual kinases that were inhibited by >85% at 10 μM to determine the corresponding Kd values. Fold of selectivity for Btk over other kinases (kinase X) is defined as Kd(kinase X)/Kd(Btk).

Cell-based functional assays

Detection of phosphor-BTK and -PLCγ2 in B cells. Human B cells were purified by RosetteSep Human B cell Enrichment Cocktail (StemCell Technologies, Vancouver, BC, Canada) according to manufacturer's instruction. $1x10^6$ cells were pre-treated with DMSO or 1 μM RN486 for 15 min followed by 5 min stimulation with goat anti-human IgM (10 μg/ml, Southern Biotech, Birmingham, AL). B Cells were pelleted and lysed in M-PER Mammalian Protein Extraction buffer (Thermo Fisher, Rockford, IL). Proteins were separated by sodium dodecyl sulfate polyacrylamide gel electrophoresis (SDS-PAGE), transferred into PVDF membranes and then blotted with mouse anti-BTK (BD Biosciences), mouse anti-phospho-BTK (Y551) (Gift from Owen Witte, UCLA), rabbit anit-PLCγ2 antibody or rabbit anti-phospho-PLCγ2 (Y1217) (both from Cell Signaling Technology, Boston, MA), and corresponding secondary antibodies.

Ramos calcium influx FLIPR assay. Ramos cells (ATCC, CRL-1596) were seeded in an assay plate, 125,000 cells per well, in phenol red free RPMI-1640 containing 2% heat inactivated FBS (Invitrogen, Carlsbad, CA), and loaded with a BD calcium dye for 1 h (Beckton Dickinson, San Jose, CA). Next, cells were treated with either RN486 or vehicle for 30 min in the dark before the plate was transferred to FLIPR Tetra (Molecular devices, Sunnyvale, CA). Immediately after the transfer and a 10 s recording

of baseline fluorescence, cells were stimulated with a mouse anti-human IgM antibody (αIgM, 10 μg/ml, clone M2E6) (Antibody Solutions Inc., Mountain View, CA) for 150 s, during which fluorescence signal was monitored and recorded. Difference between the signal and that at baseline, designated adjusted relative fluorescence unit (RFU), was calculated by using a custom Excel template to determine αIgM-induced calcium influx, and its inhibition by RN486.

B cell CD69 assay in human whole blood. Heparinized blood was freshly collected from healthy volunteers, aliquoted onto an assay plate (100 μl/well) and incubated with test compound for 30 min before the addition of goat $F(ab')_2$ anti-human IgM antibody (αIgM, final concentration 50 μg/ml) (Southern Biotech, Birmingham, AL). After a 20 h incubation, samples were added two fluorochrome-labeled mouse anti-human antibodies, one for CD20 and the other for CD69 (BD Biosciences), and further incubated for 30 min. Samples were then mixed with a lysis buffer (BD Biosciences) to remove red blood cells and washed with PBS containing 2% fetal bovine serum (FBS). Immediately after the wash, fluorescence signal for CD69 on CD20 (B cells) positive cells was acquired and analyzed, respectively, by using an LSR II flow cytometer (BD Biosciences) and a FlowJo software (Treestar, Ashland, OR).

FcγR-mediated TNFα production assay in human monocytes. Peripheral blood mononuclear cells (PBMCs) were isolated by centrifugation at 2,200 RPM from heparinized blood freshly collected from healthy volunteers. PBMCs, $1x10^5$ cells/well, were cultured in a 96 well plate for 1 to 2 h to allow monocytes to adhere. After the removal of non-adherent cells, monocytes were incubated with test compound alone for 30 min and then with human IgG coated beads (0.25 mg/ml IgG, Jackson Immunology,

JPET Fast Forward. Published on January 6, 2012 as DOI: 10.1124/jpet.111.187740
This article has not been copyedited and formatted. The final version may differ from this version.

West Grove, PA; copolymer microsphere beads, Duke Scientific, Palo Alto, CA) for 4 h. TNFα in supernatants was determined by ELISA (BD Biosciences, San Jose, CA).

Anti-4-Hydroxy-3-nitrophenylacetyl hapten (NP) IgE-induced histamine release in human mast cells. One million human cord blood derived $CD34^+$ hematopoietic stem cells (HSC; AllCells, Emeryville, CA) were cultured in a serum free StemPro-34 complete medium (Invitrogen, Carlsbad, CA) with supplements, stem cell factor (SCF; 100 ng/ml) and IL-6 (50 ng/ml). IL-3 (10 ng/ml) was also included during the first week to support cell differentiation (all cytokines from R&D Systems, Minneapolis, MN). After 8 weeks of culture, cells were stimulated with IL-4 (10 ng/ml) for 5 days. By then, most cells (90%) were differentiated into c-kit and FcεRI positive mast cells.

For measuring histamine release, 0.1 million mast cells were seeded in 96 well round bottom culture plates. Cells were sensitized with 0.1 µg/ml anti-NP IgE (Serotec, Raleigh, NC) overnight at 37 ºC. After removal of un-bound IgE, cells were treated with RN486 for 1 h, and then cross linked with 1 µg/ml NP(30)-BSA (Biosearch Technologies, Novato, CA) for 30 min at 37 ºC. A23187 or Calcimycin (Sigma; St. Louis, MO) was used as a positive control for degranulation. Supernatants were collected and assayed for histamine release by using enzyme immunoassay (EIA; Oxford Biomedical Research, Rochester Hills, MI). The percentage of histamine release was obtained by comparing with vehicle-treated mast cells with IgE-NP-crosslinking (IgE-NP, 100%).

BioMAP® profiling. To determine the profile of RN486 in more complex primary human cell systems, we had the compound tested at 0.01, 0.1, 1 and 10 µM in the BioMAP® Systems platform (BioSeek, LLC., South San Francisco, CA) across 12

BioMAP Systems containing early passage primary human cells cultured alone- or as co-cultures and stimulated with various pro-inflammatory or immunomodulatory stimuli. These systems have been previously described (Berg, et al., 2010), and include (primary human cell types/stimuli): 3C (venular endothelial cells (HuVEC)/IL-1β, TNFα and IFNγ), 4H (HuVEC/IL-4 and histamine), LPS (PBMC and HuVEC/LPS), SAg (PBMC and HuVEC/TCR ligands), BT (B cells and PBMC/anti-IgM and low levels of TCR ligands), BE3C (bronchial epithelial cells/ IL-1β, TNFα and IFNγ), BF4T (bronchial epithelial cells and human dermal fibroblasts/TNFα and IL-4), HDF3CGF (human dermal fibroblasts/ IL-1β, TNFα, IFNγ, EGF, bFGF and PDGF-BB), KF3CT (keratinocytes and dermal fibroblasts/ IL-1β, TNFα and IFNγ), CASM3C (coronary artery smooth muscle cells/ IL-1β, TNFα and IFNγ), MyoF (lung fibroblasts/TNFα and TGFβ), /Mphg (HuVEC and macrophages/TLR2). A BioMAP activity profile was generated based on the effects of test compound on the levels of various readout parameters including cytokines or growth factors, expression of surface molecules, and cell proliferation. For more technical details, see supplementary table 1.

Experimental Animals

All in vivo procedures were approved by Roche's Institutional Animal Care and Use Committee, and performed according to guidelines established by the Guide for the Care and Use of Laboratory Animals by National Research Council and by Association for the Assessment and Accreditation of Laboratory Animal Care International (AAALAC), and American Veterinary Medical Association Guidelines on Euthanasia (2007). In vivo procedures conducted at Ricerca Biosciences, LLC were approved by its institutional Animal Care and Use Committee and performed according to the same

guidelines as those followed by Roche. Animals used for the present studies were male DBA1/J, male C57BL/6 and female BALB/c mice from Jackson Laboratory (Bar Harbor, Maine), male Wistar rats, female Sprague-Dawley rats from BioLasco Taiwan (under Charles River Laboratories Technology Licensee) and female Lewis rats from Charles River Laboratories (Wilmington, MA). RN486 was synthesized at the Chemistry Department at Hoffmann La Roche in Nutley, NJ. All test compounds were dissolved in vehicle containing 0.5% hypromellose USP, 0.4% polysorbate 80 NF, 0.9% benzyl alcohol in sterile water USP with pH adjusted to 3.5 ± 0.4.

In vitro assay for CD69 in mouse splenic B cells Splenocytes were isolated from C57BL/6 mice and incubated with RN486 in a round bottom 96 well plate for 30 min before stimulation with 30 μg/ml anti-mouse IgD antibody (αIgD, LO-MD-6, Accurate Chemical & Scientific Corp, Westbury, NY) for 4 h at 37 ºC. Immediately after αIgD stimulation, cells were washed in complete RPMI and resuspended in BD FACS staining buffer at a concentration of 1×10^6 cells/100 μl. Next, cells were incubated with mouse Fc block (BD Biosciences) on ice alone for 10 min and then with fluorochrome-conjugated anti-mouse antibodies to CD69 (H1.2F3) and B220 (RA3-6B2), or corresponding isotype controls (BD Biosciences), for 20 min. Labeled cells were then washed to remove excess fluorochrome-conjugated antibodies and resuspended in BD FACS buffer. Finally, fluorescence signals for CD69 on B220 positive (B cells) cells were acquired by using an LSR II flow cytometer (BD Biosciences).

In vitro and ex vivo assays for B cell CD69 in mouse blood

Fresh whole blood was collected from mice in heparinized tubes and stimulated with αIgD (30 μg/mL) for 4 h at 37 ºC in a round bottom 96 well plate. Next, the sample

was incubated with a BD FACS lysis buffer for 10 min at room temperature to remove red blood cells. Remaining cells were washed, resuspended in BD FACS buffer, and incubated with Fc block for 10 min before being incubated with fluorochrome-conjugated antibodies for both CD69 and B220 in the dark for 30 min. Cells were then washed and resuspended in FACS buffer. Fluorescent signals for CD69 on $B220^+$ $TCR\beta^-$ cells were acquired and analyzed in the lymphocyte gate by using FlowJo (Treestar, Ashland, OR). CD69 expression in $B220^+$ cells was reported as percentage of CD69 positive/total $B220^+$ cells ($B220^+$ $CD69^+$ / $B220^+$).

The ability of RN486 to inhibit CD69 expression was examined under both in vitro and ex vivo conditions. For in vitro studies, the compound was incubated with blood for 30 min before αIgD stimulation, whereas for ex vivo experiments, the compound was administered to CIA mice as described in the section below and blood was collected at 2, 6 and 24 h post dose for αIgD stimulation.

Collagen-induced arthritis in mice

DBA1/J male mice, 7-8 weeks of age, were fed a breeder diet (Purina mouse chow #5020). After one week of acclimatization, mice received two immunizations with bovine type II antigen (100 μg each) via i.d. injection at their tail bases, first in 0.1 ml of complete Freund's adjuvant (CFA, 200 μg *mycobacterium tuberculosis* in mineral oil), and 21 days later in 0.1 ml incomplete Freund's adjuvant (IFA, neat mineral oil), for induction of arthritis. Test compound was administered orally q.d. for 14 days either preventively starting the day after the injection of IFA or therapeutically starting whenever their clinical scores reached approximately 4 (therapeutic enrollment treatment). Clinical scores, an index of arthritis, were assessed by using the following

criteria. 0= normal with no swelling or redness; 1= swelling and/or redness of paw or one digit; 2= swelling in two or more joints; 3= gross swelling of paw with more than two joints involved; 4= severe arthritis of entire paw and digits.

At the end of the study, blood was collected for ex vivo CD69 assay as described in the previous section, and for anti-type II collagen ELISA with a kit from Chondrex Inc. (Richmond, WA). Paws were collected for histopathological analysis.

Collagen antibody-induced arthritis (CAIA)

CAIA was induced in female Balb/C mice by using an Arthritogenic Kit (Chondrex Inc., Richmond, WA). Briefly, mice were injected with an anti-type II collagen antibody cocktail (4 clones, 4 mg/mouse, i.p.) on day 0 and LPS (50 μg/mouse) 3 days later. Arthritis scores are assessed by using the same criteria as those used for grading CIA.

Passive cutaneous anaphylaxis (PCA)

Male Wistar rats (5/group) weighing 140 ± 10 g were passively sensitized with a reaginic (IgE) anti-ovalbumin (anti-OVA) serum (0.05 ml/site, i.d.) at two sites on the dorsal back. As a control, one group of rats received saline instead. Animals were challenged 17 h later with ovalbumin (OVA, 1 mg per rat), which was injected i.v. along with Evans blue dye (5 mg per rat). Animals were sacrificed 30 min later and skin were photographed and collected for assessing plasma extravasation. For the purpose, skin tissues surrounding cutaneous wheals (8 mm in diameter) were biopsied by using a skin puncher. Concentrations of Evans blue, a measure of plasma extravasation, were measured at 610 nm in tissue extracts after punch tissues were incubated overnight in 2 ml of formamide at 80 °C.

JPET Fast Forward. Published on January 6, 2012 as DOI: 10.1124/jpet.111.187740
This article has not been copyedited and formatted. The final version may differ from this version.

For assessing the effect of RN486, the compound or vehicle was administered 3.5 h before OVA challenge. The effect of the compound, presented as percentage of inhibition, was determined by comparing OD610 in vehicle and compound treated animals using the following formula.

100 – [drug treatment – (-IgE)]/[vehicle control - (-IgE)] * 100.

Reverse Passive Arthus Reaction (rPAR)

Young female Sprague Dawley rats (5/group), weighing 125 ~ 130 g, were fasted overnight before the study. The animals were administered i.v. with saline containing 1% OVA (10 mg/kg) and 1% Evans blue dye 10 min before being injected i.d. with a rabbit anti-OVA IgG (50 μg/25 μl) on the left side of the back at three adjacent locations. As an isotype control, a normal rabbit IgG (50 μg/25 μl) was injected at three locations on the opposite side. As naive controls (-IgG), 5 rats received injection of saline on both sides of their backs. Vehicle or test compound was administered orally 60 min before the injection of anti-OVA IgG. Four hours after the injection, animals were euthanized with CO_2 asphyxiation for collecting skin tissues. Plasma extravasation, an index of inflammation, was determined by measuring dye extravasation in punch biopsies circumventing the injection sites (8 mm) as described in the previous section for PCA, and calculated as a difference between tissues injected with specific anti-OVA and control IgG. Percentage of inhibition is calculated using the following formula.

100 – [drug treatment – (-IgG)]/[vehicle control - (-IgG)] * 100.

Adjuvant-induced arthritis (AIA)

Complete Freund's adjuvant (CFA), a 0.5 mg *Mycobacterium butyricum* (Difco, Detroit, MI) suspension in 100 μl of mineral oil, was injected i.d. into the tail base of rats

to induce arthritis. Paw swelling, an index of arthritis, was quantified by measuring volume of hind paws using water displacement plethysmography on day 0, 7, 14 and 18. For assessing the ability of RN486 to inhibit AIA, the compound was administered to animals between day 7 and 18. As a control, vehicle was administered to two groups of rats, one with AIA and the other without. At the end of the study, spleen, hind paws and serum were collected for measurement of splenomegaly, histolopathological analysis, or profiling of serum proteins. Profiling of serum proteins was performed by using RBM RodentMAP Antigen 2 at Rules Based Medicine (Austin, TX). Samples from naïve, vehicle and 30 mg/kg RN486 groups in RN486 monotherapy and Naïve, vehicle, RN486 10 mg/kg, MTX 30 mg/kg, and RN486+MTX groups in combotherapy were included in the RBM profiling experiment, and analyzed for assessing the effects of mono- and combotherapy with RN486 and MTX on serum inflammatory markers.

Histopathological analysis

Hind paws from CIA mice or rats were collected into 10% neutral buffered formalin. After decalcification in 10% formic acid for 5 days, paws from AIA and CIA mice were embedded in paraffin and sectioned at 8 μm. Paws from rats were sectioned in the sagittal plane, whereas those from mice in the frontal plane. Tissue sections were then stained with toluidine blue. Inflammation (infiltration of inflammatory cells), pannus, cartilage damage and bone resorption were scored in a double blinded fashion by a board certified pathologist at BoulderPath, Inc (Boulder, Colorado) using their standard criteria, with 0 being normal and 5 being the most severe. For AIA rats, pannus and cartilage damage are not reported because these changes are not prominent in the model.

MicroCT imaging

MicroCT imaging was performed by an imaging specialist at Covance, Inc. (Greenfield, IN) on samples from selected groups (vehicle, 3 mg/kg and 100 mg/kg RN486) of animals in the CIA study before the samples were used for histological analysis. Data were acquired at 28 μm isotropic voxel size, photon energy of 30 KeV and current of 80 μA. Exposure time per frame was 1700 ms and the total imaging time per sample was approximately 70 min. 3-D image rendering and calculation of bone mineral density were performed using Microview (GE Healthcare, Wakesha WI).

Statistical analysis

Standard non-linear regressional analysis was performed by using custom Excel templates to determine concentration response curves and IC_{50} values in in vitro assays. The IC_{50} values reported are average from at least three studies conducted in duplicate or triplicate. For in vivo studies, one- and two-factor comparisons were performed, respectively, by using one way analysis of variance plus Dunnett's post-test and two way analysis of variance plus Bonferroni's post-test. All statistical analysis for in vivo studies was performed by using Prism 5.01 (GraphPad Software, Inc, La Jolla, CA).

Results

Potency, selectivity and pharmacokinetics of RN486. RN486 was selected from a large number of proprietary Btk inhibitors based on its potency, selectivity and pharmacokinetic profile. In the enzymatic assay, the compound potently inhibited Btk kinase activity with an IC_{50} of 4.0 nM. It binds the enzyme in a competitive manner as demonstrated in a TR-FRET based competitive binding assay with an IC_{50} of 0.3 nM. RN486 was shown to be highly selective when tested against a panel of 369 kinases in the Kinomescan. In the assay, the compound exhibited a strong and competitive binding

JPET Fast Forward. Published on January 6, 2012 as DOI: 10.1124/jpet.111.187740
This article has not been copyedited and formatted. The final version may differ from this version.

to Btk with a Kd of 0.31 nM and a high degree of selectivity over almost all other kinases including Syk and Janus kinase (JAK). The enzyme that was most potently inhibited next to Btk was Ste20 like kinase (SLK), for which the compound showed a 139 fold selectivity (Table 1). When tested in the rat and mouse, RN486 exhibited an excellent pharmacokinetic profile. In the rat, it reached the maximal concentration of 2.5 μM at 4.5 h when dosed orally at 20 mg/kg and showed a half life of 9.8 h in the blood when administered i.v.. In the mouse, the compound reached the maximal concentration of 6.0 μM at 3 h and a trough concentration of 1.0 μM at 24 h when dosed orally at 30 mg/kg.

RN486 blocks both BCR and FcR signaling. To determine the impact of Btk inhibition on BCR signaling, we examined the effects of RN486 on several key events in the BCR signaling cascade ranging from phosphorylation of Btk and PLCγ2, to calcium influx and CD69 expression in B cells with isolated human B cells, Ramos B cells, or whole blood. Stimulation with aIgM induced phosphorylation of Btk (Y551) and PLCγ2 (Y1217) in isolated B cells, calcium influx in Ramos cells and CD69 expression in blood $CD20^+$ B cells, whereas pretreatment of these cells with RN486 markedly inhibited all these signaling events, reducing both phospho-Btk and -PLCγ2 to below the baseline level without affecting the levels of total Btk or PLCγ2 (Fig. 1), and blocking calcium influx (Fig. 2A) and CD69 expression in a concentration-dependent manner, with respective IC_{50} values of 25.9 and 21.0 nM (Fig. 2B) (Table 2).

We also evaluated the ability of RN486 to block FcR-mediated responses by examining its effects on IgG-coated bead-induced TNFα release in monocytes and anti-NP IgE and antigen induced histamine release in mast cells. These responses are mediated by FcγR (Debets, et al., 1988) and FcεRI (Ishizaka, et al., 1983) respectively.

JPET Fast Forward. Published on January 6, 2012 as DOI: 10.1124/jpet.111.187740
This article has not been copyedited and formatted. The final version may differ from this version.

Addition of IgG beads to monocytes induced a significant increase in TNFα production. RN486 inhibited TNFα production in a concentration-dependent manner (Fig. 2C), with an IC_{50} of 7.0 nM (Table 2). The compound displayed a similar inhibitory effect on FcεR-mediated mast cell degranulation, reducing IgE/antigen-mediated release of histamine to the baseline level, with an average IC_{50} value of 2.9 nM (Fig. 2D and Table 2).

To examine whether RN486 was also active in mice, we assessed the effect of the compound on BCR-mediated CD69 expression in mouse splenocytes and whole blood. As in human B cell-based assays, the compound potently inhibited αIgD-stimulated CD69 expression in a dose-dependent manner in both splenic (Figs. 2E, and F) and blood B cells (Fig. 2G), with a respective IC_{50} of 2.1 ± 0.9 nM and 4.2 ± 3.2 nM (Table 2).

RN486 displays a selective B cell inhibitory profile in BioMAP Systems. Having demonstrated the ability of RN486 to potently block both BCR- and FcR-mediated biological responses in the tailored cellular assays for immunoreceptor signaling, we tested the compound in a panel of more complex primary human cell systems, namely the BioMAP Systems, that would permit us to not only further define the mechanisms of action of the compound, but also study its potential for causing off target effects (Berg, et al., 2010). The BioMAP Systems panel consists of 12 primary human mono- or co-cultures stimulated with various pro-inflammatory or immunomodulatory stimuli, including peripheral blood monocyte (PBMC) + endothelial cell (EC) co-cultures stimulated with LPS (LPS System), or super-antigen (cocktail of ligands for T cell receptor) (SAg System), and PBMC + B cell co-culture stimulated with anti-IgM and mild TCR ligands (BT System). When tested at 0.01, 0.1, 1 and 10 μM,

RN486 inhibited the proliferation of B cells, the production of IgG and cytokines (IL-2 and IL-6) in a concentration-dependent manner in the BT system without significantly affecting various readout parameters in 11 other BioMAP Systems, including the SAg and LPS Systems (Fig. 3).

RN486 blocks type I and type III hypersensitivity responses in rats. Data from cellular assays demonstrate that RN486 blocks both FcεR- and FcγR-mediated biological responses, and suggest that the compound may be effective at blocking immune hypersensitivity responses mediated by these receptors in vivo. To test this hypothesis, we assessed RN486 in rat models of PCA and rPAR. In the PCA model, a type I cutaneous hypersensitivity response was induced by passive sensitization with anti-OVA IgE (IgE, i.v.) and a subsequent challenge with the antigen OVA via i.d. injection. OVA challenge caused a severe cutaneous hypersensitivity response as demonstrated by appearance of skin wheals and dye extravasation around the sites of injection in IgE sensitized but not non-sensitized rats (Fig. 4A, top left, non-sensitized; top middle, sensitized). RN486 markedly inhibited the response, as demonstrated by the diminished wheal reaction (Fig. 4A, top right, RN486 30 mg/kg) and a dose-dependent inhibition of plasma extravasation (Fig. 4B). The maximal effect obtained is 91% (100 mg/kg), greater than the 69% inhibition noted with cyproheptadine, a non-selective anti-histamine agent used as a positive control (Fig. 4B).

In the rPAR model, a type III cutaneous hypersensitivity response was induced in reverse order to PCA by first injecting the antigen OVA (i.v.) and then anti-OVA IgG (i.d.). Anti-OVA IgG injection produced a robust inflammatory response around the site of injection, resulting in a significant increase in plasma extravasation (Fig. 4A, bottom

JPET Fast Forward. Published on January 6, 2012 as DOI: 10.1124/jpet.111.187740
This article has not been copyedited and formatted. The final version may differ from this version.

left, controls; bottom middle, vehicle treatment). Dexamethasone, a corticosteroid anti-inflammatory drug, significantly inhibited the response by ~50% (Fig. 4C). By comparison, RN486 produced a greater inhibitory effect, blocking plasma extravasation by a maximum of 75% (Fig 4A, bottom right, RN486 30 mg/kg; Fig 4C).

RN486 displays efficacy on immune arthritis induced by both active and passive immunization in mice. To determine the effect of RN486 on the development of immune arthritis, we tested the compound in two murine models of RA, namely CIA and CAIA. In the CIA model, we first tested the compound in a preventive mode. When administered orally at the doses of 3, 30 and 100 mg/kg, q.d., for 14 days starting one day after the second immunization, RN486 inhibited arthritis as measured by clinical scores in a dose-dependent manner, with a complete inhibition at 100 mg/kg, similarly to dexamethasone (Fig. 5A). When examined ex vivo, the compound almost completely inhibited αIgD-stimulated CD69 expression in blood $B220^+$ cells at 3 and 6 h post dose at all doses and by approximately 50 to 80% 24 h post dose. Under the same conditions, the compound was without effect on LPS-induced CD69 expression (Fig. 5B). RN486 also attenuated the production of anti-type II collagen antibody in a dose-dependent manner, by as much as 85% at 100 mg/kg, which is greater than the 60% inhibition by dexamethasone (Fig. 5C). The inhibitory effect on the antibody production correlates highly with that on CD69 expression noted at 24 h (r^2=0.77). Histologically, RN486 produced a dose-dependent inhibitory effect on inflammation, pannus formation, cartilage damage and bone resorption (Fig. 5D). The bone protective effect was also confirmed by microCT analysis, which revealed a marked improvement in bone density in RN486 treated mice over vehicle treated animals that displayed severe and widespread

bone loss (Fig 5E, left, vehicle; middle and right, RN486 3 and 100 mg/kg; 4F, bone mineral density of tarsal bone of hind paws).

Next, we tested RN486 in mice with established arthritis in a therapeutic dosing regimen. In the study, individual mice were randomly enrolled into either the vehicle or compound treated group when their clinical scores reached 3 to 5, and treated with RN486 (30 mg/kg, p.o., qd) consecutively for 14 days. Mice treated with vehicle displayed further increases in their clinical scores (Fig. 6A). By comparison, the progression of arthritis was completely blocked in animals treated with RN486 as demonstrated by clinical scores (Fig. 6A) and supported by histopathological analysis (Fig. 6B; Supplementary fig. 1). In contrast to preventive treatment, therapeutic dosing of RN486 resulted in only a modest and non-significant reduction in the titer of anti-type II collagen antibodies (Fig. 6C), suggesting that selective Btk inhibition attenuates arthritis development by blocking downstream effector function mediated by arthritogenic anti-type II collagen antibodies. To validate this hypothesis, we tested RN486 in the CAIA model, in which arthritis is induced by exogenous anti-type II collagen antibodies. In support of the hypothesis, the compound completely prevented anti-collagen antibody induced arthritis (Fig. 6D).

RN486 inhibits inflammation and bone erosions in adjuvant-induced arthritis either alone or in combination with methotrexate. To further validate the anti-rheumatic potential of RN486, we tested the compound in rat AIA, a standard RA model for testing small molecule anti-rheumatic and anti-inflammatory drugs such as low dose methotrexate (Welles, et al., 1985) and CP-690,550 (Tofacitinib), a new JAK inhibitor (Milici, et al., 2008). When administered alone, RN486 displayed robust and

JPET Fast Forward. Published on January 6, 2012 as DOI: 10.1124/jpet.111.187740
This article has not been copyedited and formatted. The final version may differ from this version.

dose-dependent inhibitory effects on both joint and systemic inflammation or immune response as measured by paw swelling (Fig. 7A) and splenomegaly (Fig. 7B). A maximal ~80% inhibition on paw swelling was observed at 30 mg/kg. The effect was associated with a significant suppression of histopathological changes of both inflammation and bone erosions (Fig. 7C and D; Supplementary Fig. 2). Importantly, the concentration response relationship in the model correlates with that noted in the PCA model (Fig. 7E).

Combination therapy with low dose methotrexate is an important treatment option for RA patients. We therefore determined the potential of RN486 for combined therapy with methotrexate. To identify a suboptimal or low dose of methotrexate for combination study, we tested methotrexate alone in the AIA model at doses ranging from 0.025 to 0.25 mg/kg. Methotrexate displayed a dose-dependent inhibitory effect on both paw inflammation and splenomegaly in AIA rats, attenuating paw swelling by ~50 and 100%, respectively, at 0.075 and ≥ 0.15 mg/kg (Fig. 8A).

We then tested RN486 and methotrexate at their respective suboptimal doses, namely, 10 and 0.075 mg/kg, alone or in combination in the AIA model to assess the combined effect. As in the monotherapy studies, both RN486 and methotrexate attenuated paw swelling by approximately 50% when tested alone at the suboptimal doses. When combined, the two compounds completely eradicated paw swelling (Fig. 8B), and splenomegaly (Fig. 8C), as well as histopathogical changes of inflammation and bone erosions (Fig. 8D and E).

RN486 reduces blood inflammatory markers in AIA. RA is a systemic autoimmune disease that causes inflammation not only in the joint but also systemically

as demonstrated by increased levels of acute phase response proteins and other inflammatory markers in the blood. Consequently, effective treatment of RA by using anti-rheumatic drugs in patients is frequently associated with significant reductions in serum inflammatory markers that are indicative of systemic inflammation. To investigate whether Btk inhibition also modulates serum inflammatory markers, we analyzed 59 serum protein analytes by using the RBM RodentMap panel in serum samples from both mono- and combotherapy studies with RN486. Among the 59 analytes, 23 were below the limit of detection (Supplementary table 2). Out of those (36) detected, 10 were significantly increased in vehicle treated AIA rats when compared with non-arthritic rats (Supplementary table 2), 4 of which, namely, serum C reactive protein (CRP), haptoglobin, vascular cell adhesion molecule (VCAM) and chemokine (C-C) ligand 5 (RANTES or CCL5), were significantly attenuated by both combo- and monotherapy with RN486 (Fig. 9A-D). Serum levels of these inflammatory markers correlate strongly with paw swelling as revealed by correlation analysis between paw volume and serum CRP (R^2=0.6; Fig. 9E). Among the remaining 6, five analytes, namely interferon inducible protein 10 (IP-10), monocyte chemoattractant protein-1 (MCP-1), macrophage colony stimulating factor (M-CSF), macrophage inflammatory protein-2 (MIP-2), and tissue inhibitor of metalloprotease-1 (TIMP-1), were significantly ($p<0.05$) reduced by combotherapy.

Discussion

Mutation of Btk in both humans and mice results in B cell immunodeficiency, implicating the enzyme as a key regulator of humoral immunity and a potential target for developing drugs to treat RA and other autoimmune diseases. Concordantly, we have

demonstrated that a novel Btk inhibitor RN486 blocks both BCR- and FcR-mediated hypersensitivity responses, and mitigates the development of immune arthritis in rodent models of RA.

RN486 is a reversible Btk inhibitor from a structural class distinct from previous Btk inhibitors PCI-32765 (Honigberg, et al., 2010), CGI1746 (Di Paolo, et al., 2011) and GDC-0834 (Liu, et al., 2011). In contrast to the irreversible covalent binding PCI-32765, RN486 and the two previous Btk inhibitors, CGI1746 and GDC-0834, are reversible Btk inhibitors, which are desirable for their further development as therapeutics. RN486 has an excellent potency and selectivity profile. Specifically, RN486 exhibited a subnanomolar potency for Btk and a high degree of selectivity over a large panel of 396 kinases, including Syk and JAK, two validated RA targets (Weinblatt, et al., 2010; Kremer, et al., 2009). The enzyme that was inhibited the most by RN486 next to Btk was SLK, an enzyme not implicated in autoimmune responses, with a 139 fold selectivity. Together, these data indicate that RN486 is a selective and potent inhibitor for Btk.

RN486 is able to block the signaling of BCR as demonstrated by a marked inhibition of phosphorylation of both Btk and PLCγ2 in B cells, similarly to previous Btk inhibitors (Di Paolo, et al., 2011; Honigberg, et al., 2010). Interestingly, the effect was observed in not only aIgM-stimulated, but also non-stimulated B cells, suggesting that BCR was probably already activated to a certain extent under basal experimental conditions. Importantly, the compound retained potency and selectivity in cell-based assays, strongly inhibiting key events downstream of BCR as evidenced by blockage of BCR ligand-induced calcium influx in Ramos cells and CD69 expression in the whole blood. Similarly, the compound inhibited FcR-mediated responses in effector immune

cells, abrogating mast cell degranulation and TNFα production in monocytes induced, respectively, by ligands that have been shown to specifically activate FcεRI and FcγR (Okayama, et al., 2001; Trotta, et al., 1996). RN486 is also active in mice as demonstrated by its inhibition of BCR-mediated CD69 expression in both splenic and blood B cells. In contrast, the compound failed to affect LPS-induced CD69 expression in blood, indicating that the Btk inhibitor only blocks immunoreceptor-mediated responses in immune cells.

The same holds true in more complex BioMAP primary human cell systems. Although still limited in their complexity when compared with disease tissues, the BioMAP Systems are designed to model disease environments *in vitro* by exposing primary human cells, mostly in co-culture, to combinations of disease related stimuli. More importantly, these systems have been extensively studied with a broad range of therapeutics, and shown to have the capacity for identifying mechanisms of drug actions and potential toxicities (Berg, et al., 2006; Berg, et al., 2010). In these assays, RN486 selectively inhibited the function of B cells in a BCR and TCR ligand-stimulated B cell/PBMC co-culture without affecting the function of other cell types including T cells in the same culture and macrophages stimulated with LPS. The evidence points to a specific mechanism-based inhibition of B cell activation by BCR stimulation. Also importantly, lack of effects on other cell types is consistent with the high degree of selectivity of the compound, and indicative of a low potential for RN486 to elicit off target effects.

The ability of RN486 to block immunoreceptor-mediated responses was further demonstrated in vivo in rat models of PCA and rPAR, in which the compound blocked

both type I and III hypersensitivity responses, known to be induced by FcεR-dependent mast cell degranulation, and FcγR-dependent activation of neutrophils and other innate immune cells respectively (Sakurai, et al., 2004; Ellsworth, et al., 2008). In both models, RN486 was superior to the benchmark compound cyproheptadine or dexamethasone, indicating that selective disruption of FcR signaling by inhibiting Btk is more effective than blocking distal events such as inhibiting the activity or generation of inflammatory mediators with the benchmark compounds. Together, these data unequivocally demonstrate that as in human cellular systems, Btk plays an essential role in mediating FcR-mediated responses in animal models that faithfully mimic human hypersensitivity conditions.

The same holds true in mouse models of RA, in which RN486 prevented not only the production of anti-type II collagen, but also the development of CAIA, which is mediated by FcR (Kagari, et al., 2003). At the doses (3 - 100 mg/kg) that produced efficacy in the CIA model, RN486 nearly completely inhibited ex vivo BCR ligand-induced CD69 expression for the first 6 h and by 50 – 80% at 24 h post dose. These findings are consistent with a previous report demonstrating that an approximate threshold of > 60% pBTK inhibition is required for anti-arthritic activities (Liu, et al., 2011). Importantly, CD69 inhibition at the 24 h time point correlates well with the suppression of anti-type II collagen antibody. These data suggest that a selective Btk inhibitor may produce efficacy by blocking both the production and effector function of arthritogenic antibodies that underlie the initiation and propagation of autoimmune arthritis through a selective inhibition of BCR- and FcR-signaling. Together, our findings in the mouse RA models not only confirm previous evidence for inhibition of

immune arthritis by both genetic mutation and pharmacological inhibition of Btk (Di Paolo, et al., 2011; Honigberg, et al., 2010), but also provide additional mechanistic insights through the demonstration of a strong correlation between the inhibition of arthritogenic antibodies and the suppression of BCR-dependent CD69 expression.

Besides abrogating immune arthritis in mouse CIA, which is highly dependent on B cells and humoral autoimmunity, RN486 also prevented the development of AIA, a model that is mainly driven by T cells and innate immune responses (Spargo, et al., 2006). In the model, RN486 produced not only a robust efficacy on joint inflammation and splenomegaly when dosed alone, but also a strong additive effect when combined with a low dose methotrexate. Importantly, RN486 exhibited a similar concentration response relationship in the model to that in PCA, suggesting that the concentrations required for blocking an immunoreceptor-dependent response are sufficient for efficacy. It is not clear whether BCR or FcR is involved because B cell and humoral autoimmunity have not been shown to contribute to AIA. Other possible receptors include CSF1R and MDL-1, both of which are dependent on ITAM containing DAP12 for signaling, and are implicated in immune arthritis in rodents (Huang, et al., 2009; Joyce-Shaikh, et al., 2010). Although the exact mechanism remains to be defined, our data suggest that Btk inhibitors may also produce efficacy in autoimmune conditions in which T cell and innate immune responses dominate. Importantly, evidence of an additive effect between RN486 and low dose methotrexate provides a preclinical proof of principle for potential combotherapy.

In both mono- and combotherapies, RN486 strongly protects bone in arthritic joints against erosions, indicative of disease modifying activity. Although the effect may be secondary to diminished inflammation, a Btk inhibitor may protect bone directly by

inhibiting osteoclast differentiation. This is because osteoclast differentiation in both RA models and patients is mediated by RANKL (Stolina, et al., 2005; Leibbrandt and Penninger, 2009), which requires both FcγR and CSF1R/DAP12, consequently Btk, for the action. Indeed, Btk deficiency impairs differentiation of osteoclasts from bone marrow cells stimulated with RANKL (Lee, et al., 2008). Additional studies are needed for assessing the ability of RN486 to modulate RANKL-induced osteoclast differentiation and bone resorption.

In addition to inhibiting inflammation and bone erosions, treatment with RN486 either alone or in combination significantly attenuated the levels of several serum proteins, including CRP, VCAM-1, and RANTES, in the AIA model. Interestingly, these proteins are also reduced in RA patients in response to effective anti-rheumatic therapies (Klimiuk, et al., 2007; Yang, et al., 2009). Reduction in CRP, as well as other serum proteins, in AIA correlates with improvement in paw swelling, suggesting that the proteins may be useful markers for monitoring responses to RN486. Several other proteins such as IP-10, MCP-1, MCP-3, MIP-2, TIMP-1 and VEGF, on the other hand, are only reduced by combotherapy and may be used to measure treatment responses to both RN486 and methotrexate.

In summary, we have demonstrated that a selective Btk inhibitor RN486 blocked BCR- and FcR-mediated biological and immune responses in both human cellular assays and rodent models, providing evidence for mechanism-based actions relevant to human diseases. More importantly, we demonstrated that RN486 produced a robust efficacy in two standard rodent models of RA at concentrations that effectively block immunoreceptor-mediated pharmacodynamic responses, i.e., CD69 in mice and PCA in

rats. Together, our data show that Btk is an indispensable regulator of immunoreceptor-mediated responses in both rodent and humans. Because these immunoreceptor-mediated responses are conserved between rodents and humans, and are essential for the development of immune arthritis in both species, our findings may be clinically relevant and support the development of selective Btk inhibitors as RA therapeutics.

JPET Fast Forward. Published on January 6, 2012 as DOI: 10.1124/jpet.111.187740
This article has not been copyedited and formatted. The final version may differ from this version.

Acknowledgments. We thank Aruna Raikar and her group for formulating test compounds, Jennifer Fretland for coordinating pharmacokinetic analysis and our colleagues from the Department of Comparative Medicine for supporting in vivo studies.

Authorship Contributions

Participated in research design – Xu, Vu, Liao, Pashine, Srinivasan, Kim, Postelnek, Hu, Hsu, Zhang, Narula, Hill, DeMartino, and Fine

Conducted experiments and data analysis:

CIA – Kim

AIA and CAIA – Postelnek

PCA and rPAR – Xu

Histopathology and mCT – Woods

Mouse CD69 assays - Hu, and Vu

Human cell-based assays - Hsu, Levin, Liao, Zhang, Pashine, and Srinivasan

Synthesis of RN486 and Kinomescan - Owens, and Lou

Enzymatic assay – Bradshaw, and Hill

Wrote or contributed to the writing of the manuscript: Xu, Vu, Kim, Postelnek, Hsu, Liao, Pashine, Srinivasan, DeMartino, and Fine

References

Berg EL, Kunkel EJ, Hytopoulos E and Plavec I (2006) Characterization of compound mechanisms and secondary activities by BioMAP analysis. *J Pharmacol Toxicol Methods* **53**:67-74.

Berg EL, Yang J, Melrose J, Nguyen D, Privat S, Rosler E, Kunkel EJ and Ekins S (2010) Chemical target and pathway toxicity mechanisms defined in primary human cell systems. *J Pharmacol Toxicol Methods* **61**:3-15.

Clavel C, Nogueira L, Laurent L, Iobagiu C, Vincent C, Sebbag M and Serre G (2008) Induction of macrophage secretion of tumor necrosis factor alpha through Fcgamma receptor IIa engagement by rheumatoid arthritis-specific autoantibodies to citrullinated proteins complexed with fibrinogen. *Arthritis Rheum* **58**:678-688.

Conley ME, Parolini O, Rohrer J and Campana D (1994) X-linked agammaglobulinemia: new approaches to old questions based on the identification of the defective gene. *Immunol Rev* **138**:5-21.

Debets JM, Van der Linden CJ, Dieteren IE, Leeuwenberg JF and Buurman WA (1988) Fc-receptor cross-linking induces rapid secretion of tumor necrosis factor (cachectin) by human peripheral blood monocytes. *J Immunol* **141**:1197-1201.

Di Paolo JA, Huang T, Balazs M, Barbosa J, Barck KH, Bravo BJ, Carano RA, Darrow J, Davies DR, Deforge LE, Diehl L, Ferrando R, Gallion SL, Giannetti AM, Gribling P, Hurez V, Hymowitz SG, Jones R, Kropf JE, Lee WP, Maciejewski PM, Mitchell SA, Rong H, Staker BL, Whitney JA, Yeh S, Young WB, Yu C, Zhang J, Reif K and

Currie KS (2011) Specific Btk inhibition suppresses B cell- and myeloid cell-mediated arthritis. *Nat Chem Biol* **7**:41-50.

Edwards JC, Leandro MJ and Cambridge G (2005) B lymphocyte depletion in rheumatoid arthritis: targeting of CD20. *Curr Dir Autoimmun* **8**:175-192.

Ellsworth JL, Maurer M, Harder B, Hamacher N, Lantry M, Lewis KB, Rene S, Byrnes-Blake K, Underwood S, Waggie KS, Visich J and Lewis KE (2008) Targeting immune complex-mediated hypersensitivity with recombinant soluble human FcgammaRIA (CD64A). *J Immunol* **180**:580-589.

Fabian MA, Biggs WH, III, Treiber DK, Atteridge CE, Azimioara MD, Benedetti MG, Carter TA, Ciceri P, Edeen PT, Floyd M, Ford JM, Galvin M, Gerlach JL, Grotzfeld RM, Herrgard S, Insko DE, Insko MA, Lai AG, Lelias JM, Mehta SA, Milanov ZV, Velasco AM, Wodicka LM, Patel HK, Zarrinkar PP and Lockhart DJ (2005) A small molecule-kinase interaction map for clinical kinase inhibitors. *Nat Biotechnol* **23**:329-336.

Honigberg LA, Smith AM, Sirisawad M, Verner E, Loury D, Chang B, Li S, Pan Z, Thamm DH, Miller RA and Buggy JJ (2010) The Bruton tyrosine kinase inhibitor PCI-32765 blocks B-cell activation and is efficacious in models of autoimmune disease and B-cell malignancy. *Proc Natl Acad Sci U S A* **107**:13075-13080.

Huang H, Hutta DA, Rinker JM, Hu H, Parsons WH, Schubert C, DesJarlais RL, Crysler CS, Chaikin MA, Donatelli RR, Chen Y, Cheng D, Zhou Z, Yurkow E, Manthey CL and Player MR (2009) Pyrido[2,3-d]pyrimidin-5-ones: a novel class of

antiinflammatory macrophage colony-stimulating factor-1 receptor inhibitors. *J Med Chem* **52**:1081-1099.

Ishizaka T, Conrad DH, Schulman ES, Sterk AR and Ishizaka K (1983) Biochemical analysis of initial triggering events of IgE-mediated histamine release from human lung mast cells. *J Immunol* **130**:2357-2362.

Jansson L and Holmdahl R (1993) Genes on the X chromosome affect development of collagen-induced arthritis in mice. *Clin Exp Immunol* **94**:459-465.

Joyce-Shaikh B, Bigler ME, Chao CC, Murphy EE, Blumenschein WM, Adamopoulos IE, Heyworth PG, Antonenko S, Bowman EP, McClanahan TK, Phillips JH and Cua DJ (2010) Myeloid DAP12-associating lectin (MDL)-1 regulates synovial inflammation and bone erosion associated with autoimmune arthritis. *J Exp Med* **207**:579-589.

Kagari T, Tanaka D, Doi H and Shimozato T (2003) Essential role of Fc gamma receptors in anti-type II collagen antibody-induced arthritis. *J Immunol* **170**:4318-4324.

Klimiuk PA, Fiedorczyk M, Sierakowski S and Chwiecko J (2007) Soluble cell adhesion molecules (sICAM-1, sVCAM-1, and sE-selectin) in patients with early rheumatoid arthritis. *Scand J Rheumatol* **36**:345-350.

Koga T, Inui M, Inoue K, Kim S, Suematsu A, Kobayashi E, Iwata T, Ohnishi H, Matozaki T, Kodama T, Taniguchi T, Takayanagi H and Takai T (2004) Costimulatory signals mediated by the ITAM motif cooperate with RANKL for bone homeostasis. *Nature* **428**:758-763.

Kremer JM, Bloom BJ, Breedveld FC, Coombs JH, Fletcher MP, Gruben D, Krishnaswami S, Burgos-Vargas R, Wilkinson B, Zerbini CA and Zwillich SH (2009) The safety and efficacy of a JAK inhibitor in patients with active rheumatoid arthritis: Results of a double-blind, placebo-controlled phase IIa trial of three dosage levels of CP-690,550 versus placebo. *Arthritis Rheum* **60**:1895-1905.

Kurosaki T (2000) Functional dissection of BCR signaling pathways. *Curr Opin Immunol* **12**:276-281.

Kurosaki T, Maeda A, Ishiai M, Hashimoto A, Inabe K and Takata M (2000) Regulation of the phospholipase C-gamma2 pathway in B cells. *Immunol Rev* **176**:19-29.

Lee SH, Kim T, Jeong D, Kim N and Choi Y (2008) The tec family tyrosine kinase Btk Regulates RANKL-induced osteoclast maturation. *J Biol Chem* **283**:11526-11534.

Leibbrandt A and Penninger JM (2009) RANKL/RANK as key factors for osteoclast development and bone loss in arthropathies. *Adv Exp Med Biol* **649**:100-113.

Liu L, Di PJ, Barbosa J, Rong H, Reif K and Wong H (2011) Antiarthritis Effect of a Novel Bruton's Tyrosine Kinase (BTK) Inhibitor in Rat Collagen-Induced Arthritis and Mechanism-Based Pharmacokinetic/Pharmacodynamic Modeling: Relationships between Inhibition of BTK Phosphorylation and Efficacy. *J Pharmacol Exp Ther* **338**:154-163.

Milici AJ, Kudlacz EM, Audoly L, Zwillich S and Changelian P (2008) Cartilage preservation by inhibition of Janus kinase 3 in two rodent models of rheumatoid arthritis. *Arthritis Res Ther* **10**:R14.

Mullazehi M, Mathsson L, Lampa J and Ronnelid J (2007) High anti-collagen type-II antibody levels and induction of proinflammatory cytokines by anti-collagen antibody-containing immune complexes in vitro characterise a distinct rheumatoid arthritis phenotype associated with acute inflammation at the time of disease onset. *Ann Rheum Dis* **66**:537-541.

Nimmerjahn F and Ravetch JV (2008) Fcgamma receptors as regulators of immune responses. *Nat Rev Immunol* **8**:34-47.

Okayama Y, Hagaman DD, Woolhiser M and Metcalfe DD (2001) Further characterization of FcgammaRII and FcgammaRIII expression by cultured human mast cells. *Int Arch Allergy Immunol* **124**:155-157.

Sakurai D, Yamasaki S, Arase K, Park SY, Arase H, Konno A and Saito T (2004) Fc epsilon RI gamma-ITAM is differentially required for mast cell function in vivo. *J Immunol* **172**:2374-2381.

Schaller M, Stohl W, Tan SM, Benoit VM, Hilbert DM and Ditzel HJ (2005) Raised levels of anti-glucose-6-phosphate isomerase IgG in serum and synovial fluid from patients with inflammatory arthritis. *Ann Rheum Dis* **64**:743-749.

Spargo LD, Cleland LG, Cockshell MP and Mayrhofer G (2006) Recruitment and proliferation of CD4+ T cells in synovium following adoptive transfer of adjuvant-induced arthritis. *Int Immunol* **18**:897-910.

Stolina M, Adamu S, Ominsky M, Dwyer D, Asuncion F, Geng Z, Middleton S, Brown H, Pretorius J, Schett G, Bolon B, Feige U, Zack D and Kostenuik PJ (2005) RANKL

is a marker and mediator of local and systemic bone loss in two rat models of inflammatory arthritis. *J Bone Miner Res* **20**:1756-1765.

Thomas JD, Sideras P, Smith CI, Vorechovsky I, Chapman V and Paul WE (1993) Colocalization of X-linked agammaglobulinemia and X-linked immunodeficiency genes. *Science* **261**:355-358.

Trotta R, Kanakaraj P and Perussia B (1996) Fc gamma R-dependent mitogen-activated protein kinase activation in leukocytes: a common signal transduction event necessary for expression of TNF-alpha and early activation genes. *J Exp Med* **184**:1027-1035.

Weinblatt ME, Kavanaugh A, Genovese MC, Musser TK, Grossbard EB and Magilavy DB (2010) An oral spleen tyrosine kinase (Syk) inhibitor for rheumatoid arthritis. *N Engl J Med* **363**:1303-1312.

Welles WL, Silkworth J, Oronsky AL, Kerwar SS and Galivan J (1985) Studies on the effect of low dose methotrexate on rat adjuvant arthritis. *J Rheumatol* **12**:904-906.

Yang MH, Wu FX, Xie CM, Qing YF, Wang GR, Guo XL, Tang Z, Zhou JG and Yuan GH (2009) Expression of CC chemokine ligand 5 in patients with rheumatoid arthritis and its correlation with disease activity and medication. *Chin Med Sci J* **24**:50-54.

Zhao X, Okeke NL, Sharpe O, Batliwalla FM, Lee AT, Ho PP, Tomooka BH, Gregersen PK and Robinson WH (2008) Circulating immune complexes contain citrullinated fibrinogen in rheumatoid arthritis. *Arthritis Res Ther* **10**:R94.

Legends for figures

Figure 1. Inhibition of Btk and PLCγ2 phosphorylation by RN486. RN486 inhibited phosphor-Btk (Y551) and PLCγ2 (Y1217), but not total Btk or PLCγ2 in both non- and anti-IgM-stimulated human B cells.

Figure 2. Functional activity of RN486 in cell-based assays. A, Inhibition of calcium influx induced by αIgM, a BCR agonist, in Ramos cells. Intracellular calcium concentrations were measured by using a calcium sensitive fluorescent dye and presented as adjusted relative fluorescence units (RFU). B, Inhibition of αIgM-induced CD69 expression in $CD20^+$ cells in human whole blood. CD69 expression in $CD20^+$ cells was analyzed by using FACS and presented as % of $CD20^+$ cells that expresses CD69. C, Inhibition of TNFα production in monocytes induced by IgG coated beads. D, Inhibition of histamine release in human mast cells induced by anti-NP IgE and NP. Human mast cells derived from cord stem cells showed a modest (5-10%) release of histamine (cell only). Anti-NP IgE and NP crosslinking-induced a robust histamine release, which is indicated as 100%, slightly lower than that (112%) induced by calcium ionophore A23187, a positive control for causing a maximum of histamine release. RN486 attenuated IgE-NP induced histamine release in a concentration-dependent manner, reducing it to near baseline levels at the maximal concentration tested. E, FACS analysis of CD69 expression in mouse $B220^+$ splenic B cells by RN486. Mean fluorescence intensity on X- and Y-axis represents, respectively, the density of cells expressing CD69 and B220. Percentage of $CD69^+$ $B220^+$ cells (boxed) was reduced by RN486 in a dose-dependent manner. F and G, Inhibition of CD69 expression in $B220^+$ cells (% of $CD69^+$

$B220^+$) by RN486 in mouse splenic (F) and blood (G) B cells. The compound dose-dependently attenuated αIgD-stimulated CD69 expression in $B220^+$ cells, returning the expression to baseline (unstim) levels at the highest concentrations. Data are reported as average values of replicate or triplicate.

Figure 3. Selective inhibition of B cell functions across a panel of BioMAP primary human multi-cellular systems. The biomarker readouts measured in each System are indicated along the x-axis. The y-axis shows the $\log_{10}$ expression ratios of the readout level measurements relative to solvent (DMSO buffer) controls. Each data point represents a single well. The grey area above and below the y-axis origin indicates the 95% significance envelope of DMSO negative controls. RN486 inhibited proliferation of B cells, production of IgG and cytokines (TNFα, IL-6 and IL-2) in a co-culture of B cells and PBMCs exposed to BCR and TCR ligands (BT System) without affecting the function of other cell types including T cells in the multi-cellular systems (SAg and LPS Systems). In contrast, RN486 was without effects on the other BioMAP Systems containing various primary human cells including endothelial, fibroblast, myeloid and epithelial cell types.

Figure 4. Inhibition of immune hypersensitivity responses by RN486. A, Representative images from selected treatment groups to depict attenuation of plasma extravasation by RN486 in the PCA model (top panel, left – non-sensitized control; middle – vehicle; right – RN486 30 mg/kg) and the rPAR model (bottom panel, left – non-sensitized control; middle – vehicle; right - RN486 30 mg/kg). B and C, Dose response of RN486

in PCA (B) and rPAR (C). Data are presented as percentage of plasma extravasation relative to vehicle (100%) and non-sensitized controls (0%, -IgE in B; -IgG in C). Cyproheptadine (Cyp) and dexamethasone (Dex) were used in the experiments as positive controls. (n=5/group; **, $p<0.01$ vs. vehicle).

Figure 5. Anti-inflammatory and disease modifying effects of RN486 in the mouse CIA model. A, Dose-dependent attenuation of clinical scores by RN486 (n=14/group). B, Inhibition of αIgD, but not, LPS-induced CD69 expression in ex vivo whole blood assay at 24 h post dose. CD69 expression in $B220^{+}$ cells was induced ex vivo with αIgD or LPS in terminal whole blood from subgroups of mice 24 h post dose. CD69 expression in non-stimulated (-αIgD) was also examined and used as a baseline control. N=5/group. C, Attenuation of plasma levels of anti-type II collagen antibody (total IgG) by RN486 and dexamethasone. D, Histopathological analysis of inflammation, pannus formation, cartilage damage and bone resorption in the hind paws of a subgroup of mice (n=7/group). E, Representative microCT images from a vehicle (left) or RN486 treated mouse (middle - 3 mg/kg; right – 100 mg/kg) depicting the bone protective effect of RN486. F, Quantitative analysis of bone mineral density in tarsal bone of hind paws from a region of interest (3.2 x 1.2 x 2.2 mm) in the mCT images (n=7/group). *, $p<0.05$ and **, $p<0.01$ when compared with vehicle treated group.

Figure 6. Inhibitory effect of RN486 on the effector phase of immune arthritis in mice. A-C, Inhibitory effects in the CIA model on clinical scores (A), histopathological changes in inflammation, pannus, cartilage damage and bone resorption (B) and plasma

levels of anti-type II collagen Ab (C). n=12/group for vehicle and 14/group for RN486. D, Inhibitory effect on clinical scores in the CAIA model. N=6 for vehicle; 8/group for RN486. **, $p<0.01$ vs. vehicle.

Figure 7. Anti-inflammatory and disease modifying effects of RN486 in the rat AIA model. A, Inhibition of paw swelling by RN486. B, Attenuation of splenomegaly by RN486. C, Histopathological analysis of inflammation. D, Histopathological analysis of bone erosions. E, Correlation in the concentration response relationship between PCA and AIA models. N=6-7/group except for –AIA with n=3/group. *, $p<0.05$; **, $p<0.01$ vs. vehicle.

Figure 8. Additive inhibitory effects of RN486 and methotrexate (MTX) on inflammation and bone erosions in the rat AIA model. A, Inhibition of paw swelling by methotrexate alone. B-E, Inhibition of paw swelling (B), splenomegaly (C), inflammation (D) and bone resorption (E) by suboptimal doses of RN486 and methotrexate alone or in combination. N=6/group except for –AIA with n=3/group. *, $p<0.05$; **, $p<0.01$ vs. vehicle.

Fig 9. Inhibitory effects of RN486, alone or in combination with methotrexate, on serum inflammatory markers in the AIA model alone or in combination with methotrexate. N=5 – 10/group; *, $p<0.05$; **, $p<0.01$ vs. vehicle.

JPET Fast Forward. Published on January 6, 2012 as DOI: 10.1124/jpet.111.187740
This article has not been copyedited and formatted. The final version may differ from this version.

Table 1. Potency and selectivity profile of RN486 in enzymatic assays

	Btk	SLK	TEC	FGR	ITK	ABL1	YES	LCK	JAK1
Kd (μM)	0.00031	0.043	0.064	0.1	0.24	0.29	0.38	0.86	5.1
Selectivity	1	139	206	323	774	935	1226	2774	16452

JPET Fast Forward. Published on January 6, 2012 as DOI: 10.1124/jpet.111.187740
This article has not been copyedited and formatted. The final version may differ from this version.

Table 2. Potency of RN486 in cell-based assays

	BCR signaling				FcR signaling	
Assays	Ramos ($Ca2^{+}$)	Human whole blood (CD69)	Mouse whole blood (CD69)	Mouse splenocytes (CD69)	Mast cell (histamine)	Monocytes (TNFα)
IC_{50} (nM)	25.9 ± 10.9 (5)	21.0 ± 1.3 (75)	4.2 ± 3.2 (8)	2.1 ± 0.9 (8)	2.9 ± 2.3 (3)	7.0± 2.0 (3)

Values are mean ± SEM for the IC_{50} values for several experiments, with (n) = number of experiments.

JPET Fast Forward. Published on January 6, 2012 as DOI: 10.1124/jpet.111.187740
This article has not been copyedited and formatted. The final version may differ from this version.

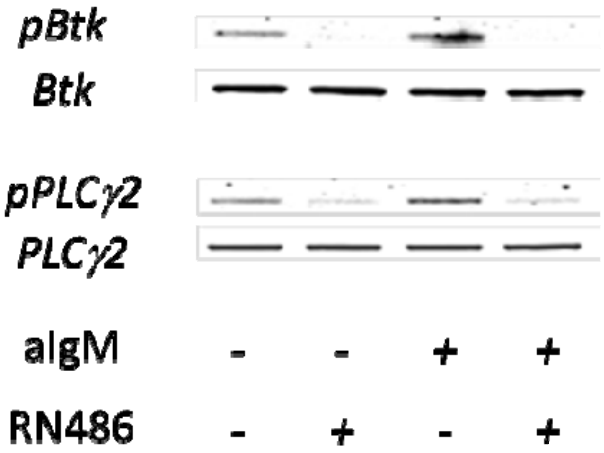

Figure 1

JPET Fast Forward. Published on January 6, 2012 as DOI: 10.1124/jpet.111.187740
This article has not been copyedited and formatted. The final version may differ from this version.

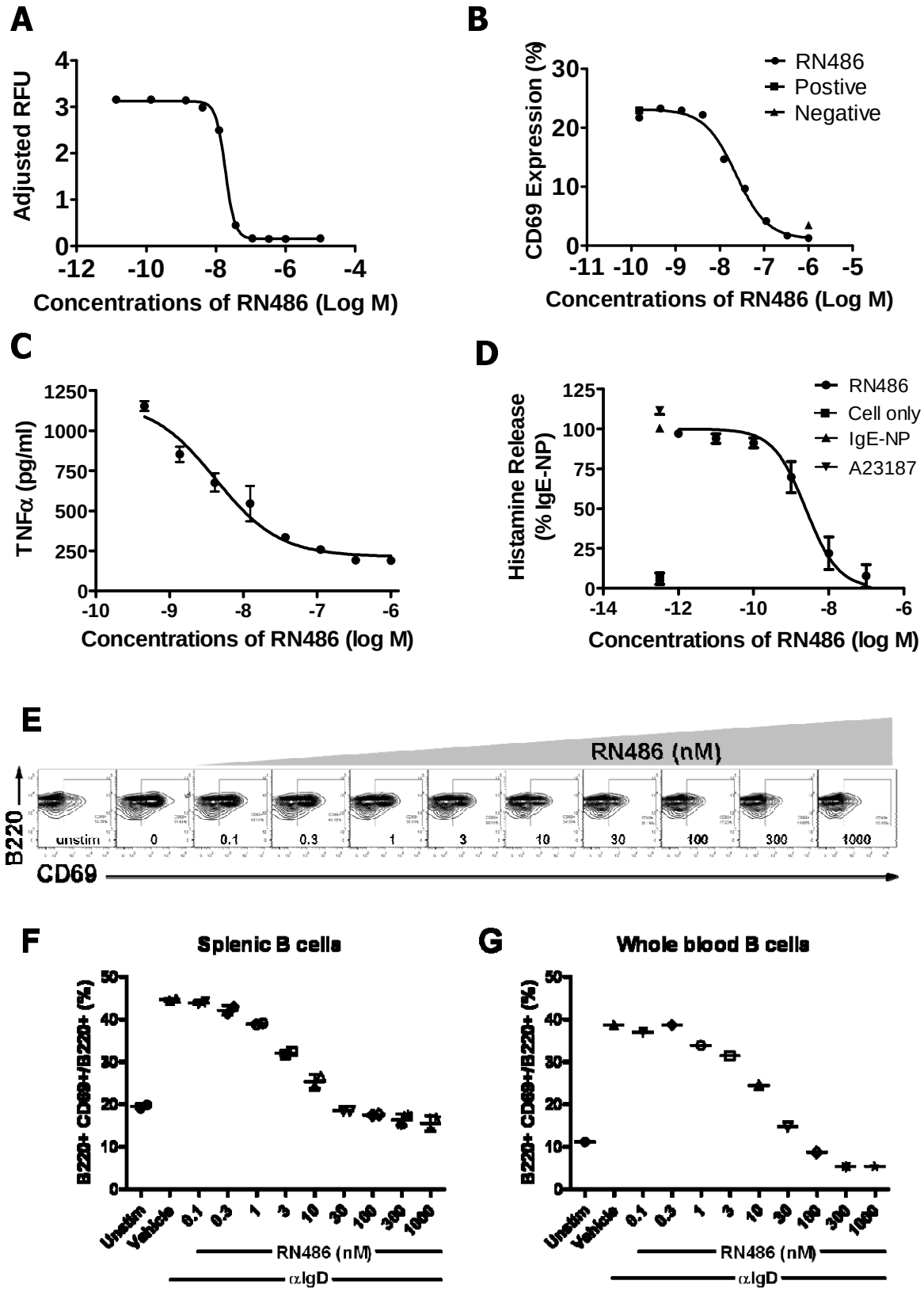

Figure 2

JPET Fast Forward. Published on January 6, 2012 as DOI: 10.1124/jpet.111.187740
This article has not been copyedited and formatted. The final version may differ from this version.

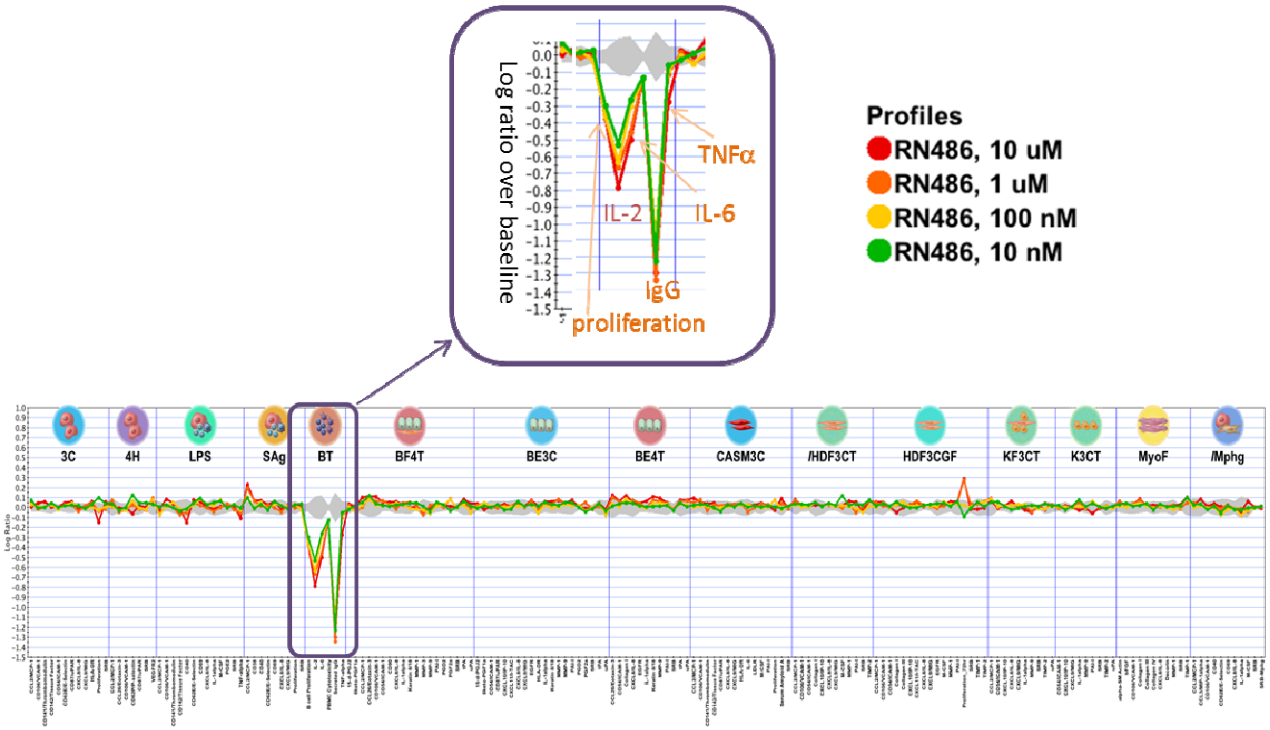

Figure 3

JPET Fast Forward. Published on January 6, 2012 as DOI: 10.1124/jpet.111.187740
This article has not been copyedited and formatted. The final version may differ from this version.

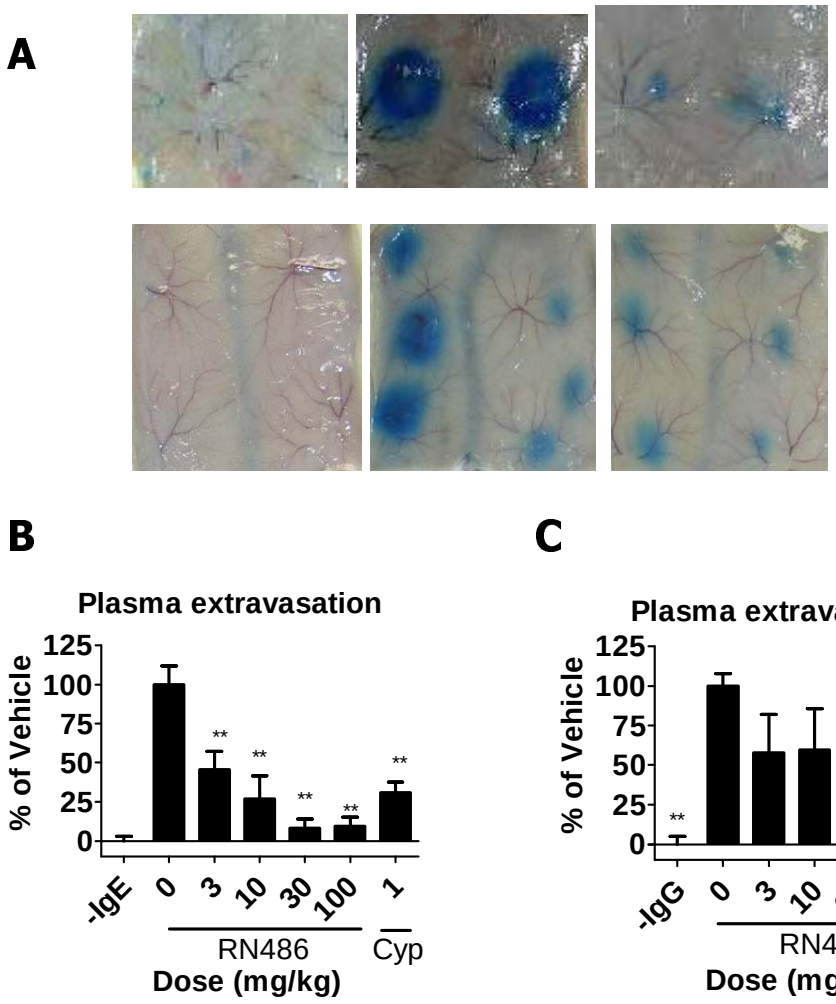

Figure 4

JPET Fast Forward. Published on January 6, 2012 as DOI: 10.1124/jpet.111.187740
This article has not been copyedited and formatted. The final version may differ from this version.

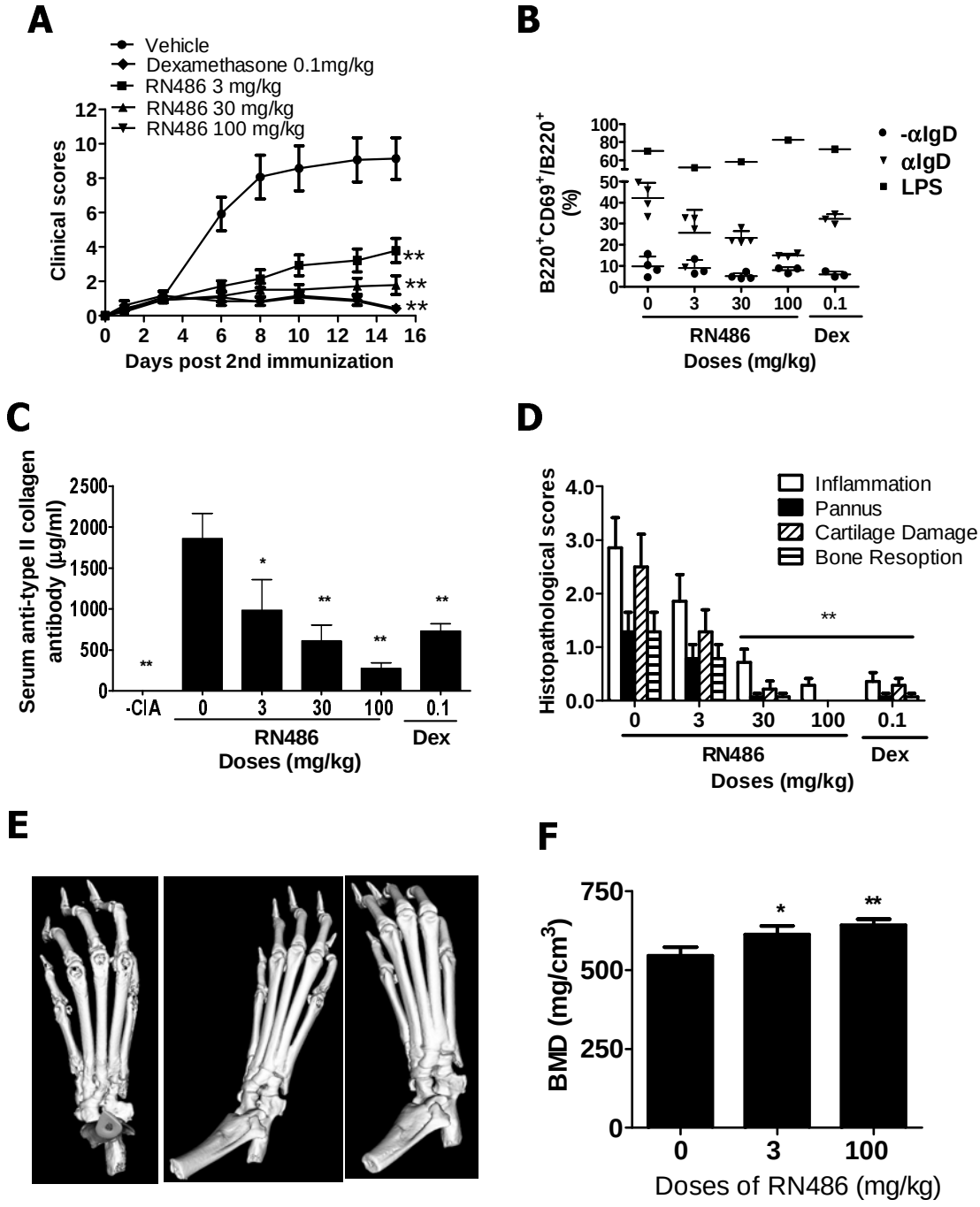

Figure 5

JPET Fast Forward. Published on January 6, 2012 as DOI: 10.1124/jpet.111.187740
This article has not been copyedited and formatted. The final version may differ from this version.

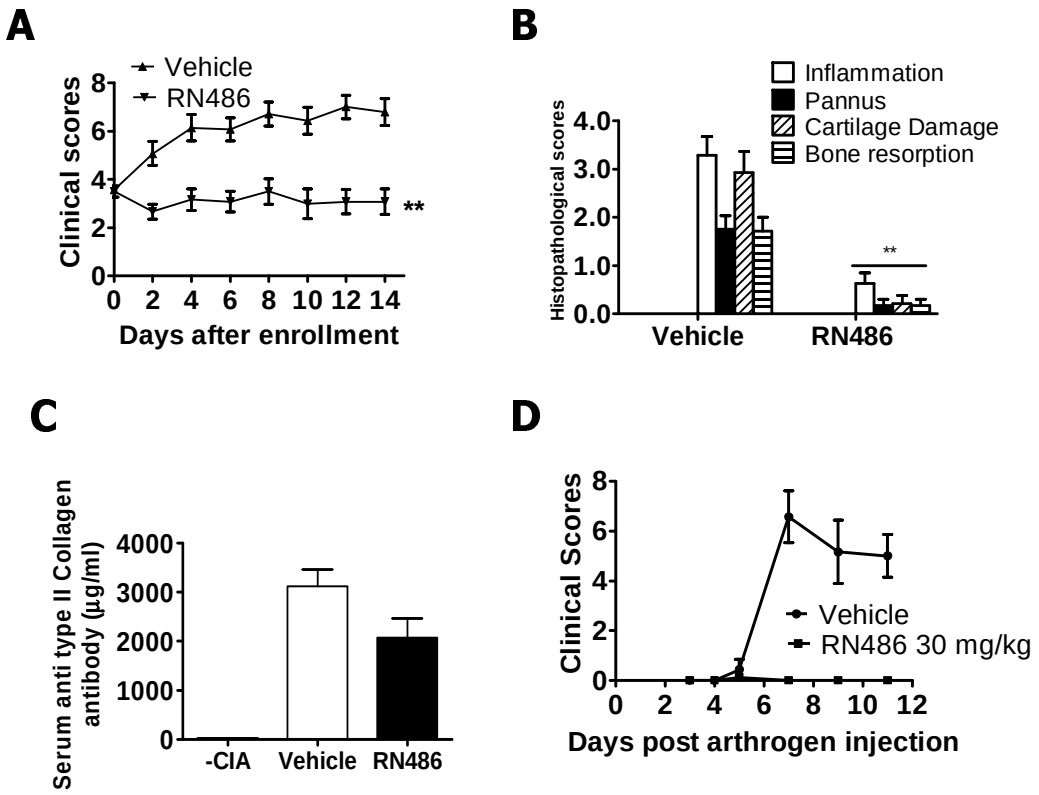

Figure 6

JPET Fast Forward. Published on January 6, 2012 as DOI: 10.1124/jpet.111.187740
This article has not been copyedited and formatted. The final version may differ from this version.

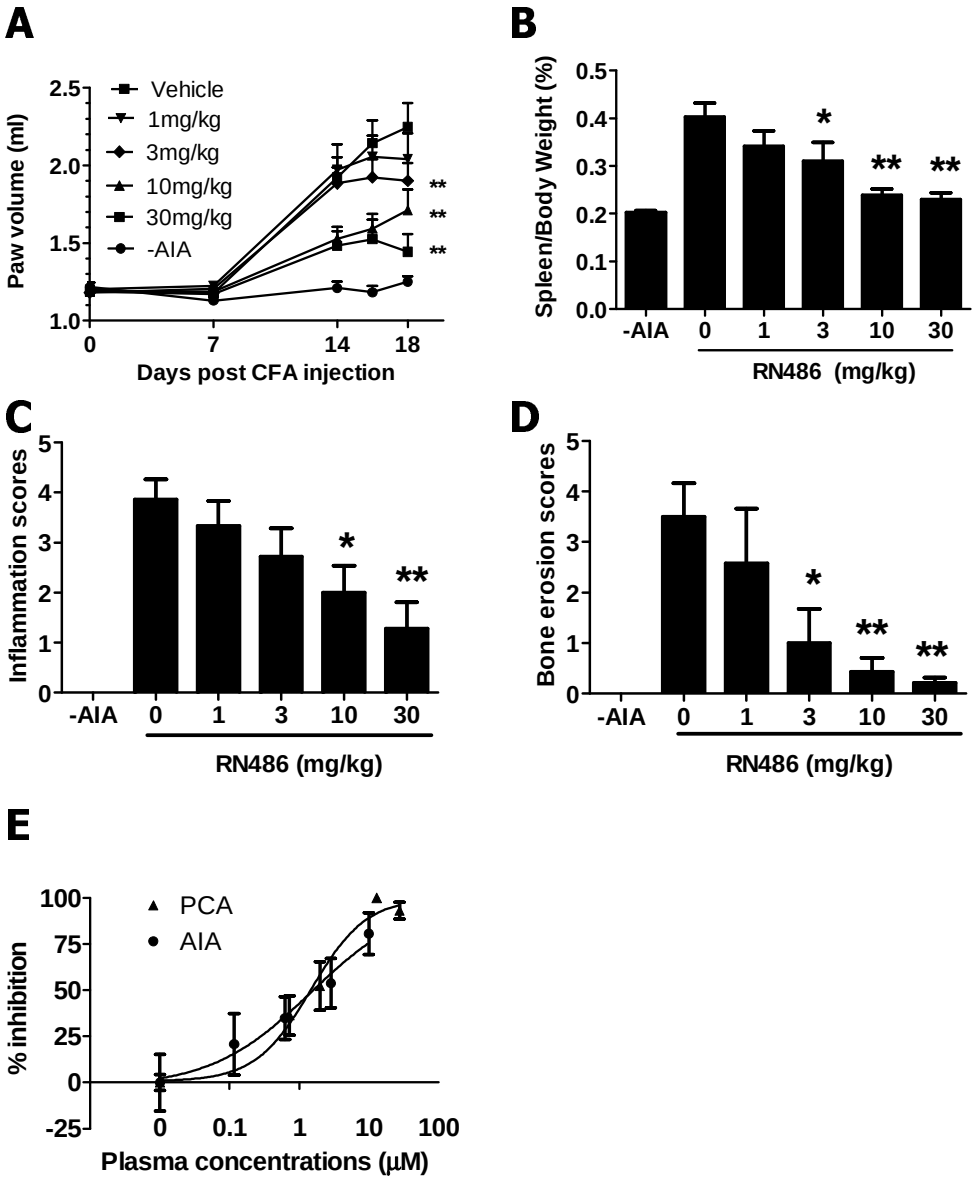

Figure 7

JPET Fast Forward. Published on January 6, 2012 as DOI: 10.1124/jpet.111.187740
This article has not been copyedited and formatted. The final version may differ from this version.

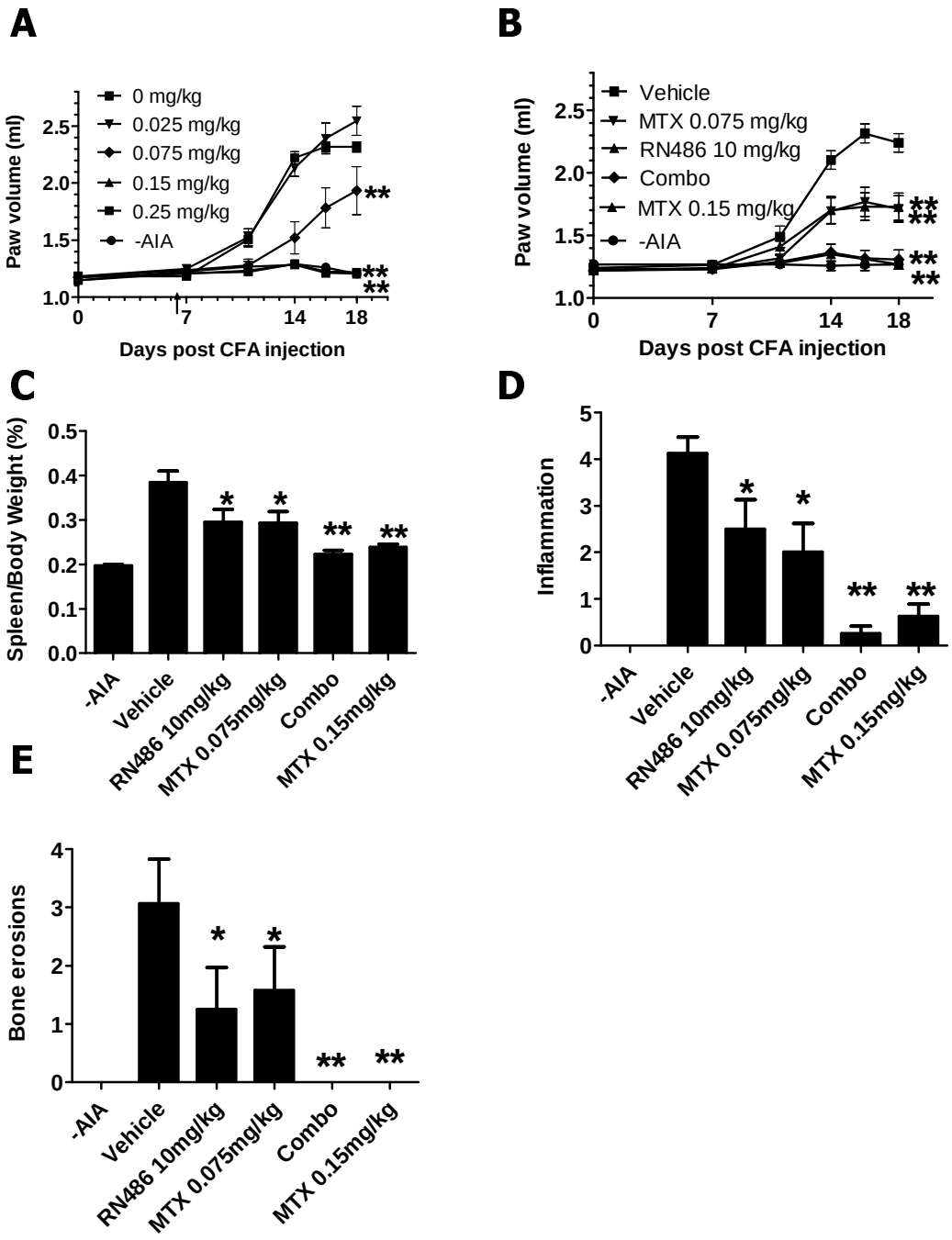

Figure 8

JPET Fast Forward. Published on January 6, 2012 as DOI: 10.1124/jpet.111.187740
This article has not been copyedited and formatted. The final version may differ from this version.

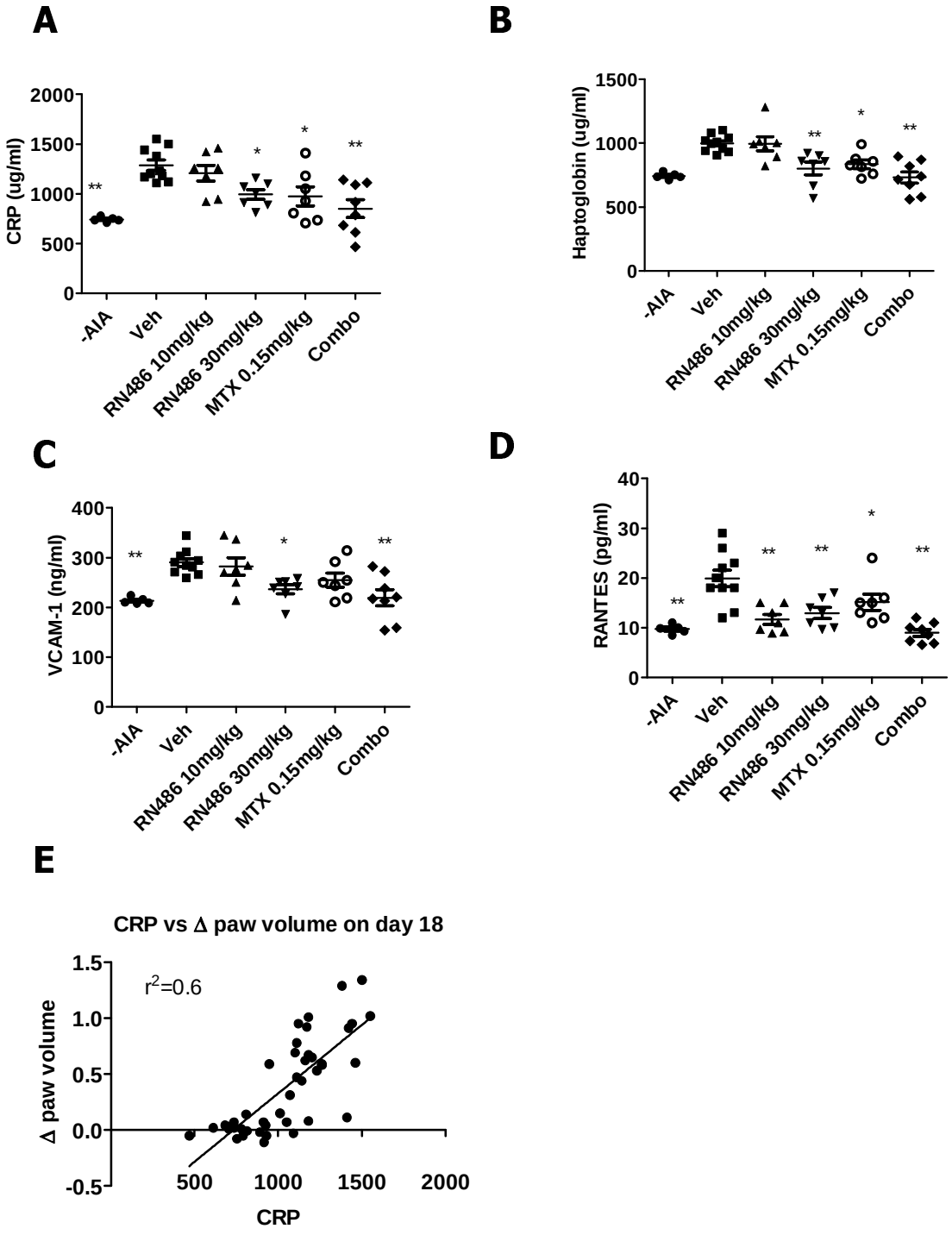

Figure 9